The Simplest Layer-by-Layer Assembly Structure: Best Paired Polymer Electrolytes with One Charge per Main Chain Carbon Atom for Multilayered Thin Films

ARTICLE *in* MACROMOLECULES · APRIL 2010

Impact Factor: 5.8 · DOI: 10.1021/ma100473j

8 AUTHORS, INCLUDING:

Tsuyoshi Michinobu
Tokyo Institute of Technology
128 PUBLICATIONS **2,684** CITATIONS
SEE PROFILE

Jonathan P Hill
National Institute for Materials Science
286 PUBLICATIONS **8,686** CITATIONS
SEE PROFILE

Seimei Shiratori
Keio University
121 PUBLICATIONS **4,061** CITATIONS
SEE PROFILE

Katsuhiko Ariga
National Institute for Materials Science
623 PUBLICATIONS **21,611** CITATIONS
SEE PROFILE

Macromolecules
ARTICLE

Macromolecules **2010**, *43*, 3947–3955 **3947**
DOI: 10.1021/ma100473j

The Simplest Layer-by-Layer Assembly Structure: Best Paired Polymer Electrolytes with One Charge per Main Chain Carbon Atom for Multilayered Thin Films

Nozomu Fujii,[†] Kouji Fujimoto,[‡] Tsuyoshi Michinobu,[†,§] Misaho Akada,[⊥] Jonathan P. Hill,[⊥] Seimei Shiratori,*[,‡] Katsuhiko Ariga,*[,⊥] and Kiyotaka Shigehara*[,†]

[†]*Graduate School of Engineering, Tokyo University of Agriculture and Technology, Koganei, Tokyo 184-8588, Japan,* [‡]*Faculty of Science and Technology, Keio University, Yokohama 223-8522, Japan,* [§]*Global Edge Institute, Tokyo Institute of Technology, Ookayama, Meguro-ku, Tokyo 152-8550, Japan, and* [⊥]*World Premier International (WPI) Research Center for Materials Nanoarchitectonics (MANA), National Institute for Materials Science (NIMS) and JST, CREST, 1-1 Namiki, Tsukuba 305-0044, Japan*

Received March 1, 2010; Revised Manuscript Received March 10, 2010

ABSTRACT: Layer-by-layer (LbL) thin film assembly behaviors of the polymethylene-type polyelectrolytes poly(fumaric acid) and poly(methyleneamine) were comprehensively studied as a function of the dipping solution pH values. Since polymethylene-type polyelectrolytes can possess double the density of side-chain charges of conventional vinyl (or polyethylene-type) polyelectrolytes, they exhibited stronger intramolecular side-chain interactions, which were revealed by potentiometric titrations and their sequential adsorption behaviors. Thicknesses of the LbL thin films obtained decreased with the degree of ionization of both polyelectrolytes. The pH-dependent variation in film thickness was subtle and continuous when compared with the vinyl polyelectrolytes, probably because of the large variation in pK_a of the polymethylene-type polyelectrolytes in the multilayer thin films. Refractive indices of the thin films were not positively correlated with their thicknesses, but the pH matrix displayed maximum values for the combination of almost fully charged polycation and polyanion. The main chains of highly charged polyelectrolytes are apparently substantially extended, resulting in the optimal packing of polycations and polyanions, in terms of the electrostatic attractions, to form high-density polymer films. AFM measurements revealed that the high-density thin films are composed of densely assembled almost monodispersed polymer nanoparticles with an average diameter of 17 nm. In contrast, flexible polymers with fewer side-chain charges are loosely assembled, giving thicker films of relatively low density. Thus, the pH matrix of the refractive indices is inversely correlated with that of the roughness parameters determined by AFM measurements. Finally, FT-IR-RAS spectra revealed the presence of charged species in all the LbL thin films, suggesting a significantly decreased pK_a for poly(fumaric acid). These results illustrate some of the most fundamental and unexplored aspects of LbL film assemblies based on the simplest of chemical structures.

Introduction

Since the layer-by-layer (LbL) technique was established over a decade ago,[1] the alternating assembly of oppositely charged polyelectrolyes has become a versatile method for preparation of ultrathin multilayer films of variable thickness, composition, and function. Because of the simplicity of the assembly process, a wide variety of charged materials including synthetic polymers,[2] biomaterials,[3] supramolecular assemblies,[4] carbon-based nanomaterials,[5] and inorganic substances[6] can be incorporated into the ultrathin films. In particular, the excellent compatibility of LbL methods with biological interfaces has enabled numerous important applications such as biocatalysis, toxicity screening, and drug delivery systems.[7] Thus, recent trends in research on LbL techniques has been largely directed at development of novel and practical applications.

Fundamental research on the LbL assembly process has been in the past performed independently for strong and weak polyelectrolytes and sometimes their combinations.[8] In the case of strong polyelectrolytes, modulation of ionic strength by addition of salt to the aqueous dipping solutions was found to be a key factor in controlling the film thickness of the adsorbed layers.[9] On the other hand, film thickness control of assembled weak polyelectrolytes can be achieved by simply adjusting the dipping solution pH values. This simplicity is one of the notable advantages for the use of weak polyelectrolytes in technological LbL applications, and the pH effects on the resultant LbL thin films have been comprehensively summarized.[10] Very thick bilayers are usually obtained by the combination of fully ionized polycation and nearly fully ionized polyanion or vice versa. Hydrogen bonding is also regarded as an important secondary factor.[11] However, if we consider the chemical structures of the polyelectrolytes used, the previous systematic studies have always been carried out with typical vinyl polyelectrolytes, such as poly(acrylic acid) and poly(allylamine), although some copolymers have led to more complicated analytical results. It is remarkable that other fundamental polymer structures have not been applied for preparing LbL assemblies. In particular, the critical question of what happens if the charge density per molecule of polyelectrolytes is increased beyond that of the currently popular vinyl polyelectrolytes should be addressed. Ideally, charge density should reach one charge per carbon atom of the polymer main chain. Answering this kind of fundamental question will lead to accumulation of scientific knowledge and the further development of LbL science and the technology.

One of our groups has been continuing a project on the synthesis of functionalized polymethylene-type polymers. Recent

*Corresponding authors. E-mail: jun@cc.tuat.ac.jp (K.S.), ARIGA.Katsuhiko@nims.go.jp (K.A.), shiratori@appi.keio.ac.jp (S.S.).

Published on Web 03/17/2010

Chart 1. Chemical Structures of Polymethylene-Type Polyelectrolytes, PF and PMA

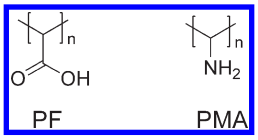

examples include a series of side-chain liquid crystalline poly(fumarate)s,[12] and the fundamental polymer structure of poly(fumaric acid) (PF) is readily accessible. PF can serve as a polyanion with the simplest repeat unit and highest charge density of the hitherto accessible polyanions (Chart 1). Fortunately, the counter polymethylene-type polycation, poly(methyleneamine) (PMA), was recently reported.[13] However, until now neither of these polymers had been applied in the LbL technique. Assembly behavior of these polymers is expected to be strongly influenced by the rigidity of single polymer main chains as well as enhanced electrostatic interactions. If mechanical strength and thermal stability of the resultant LbL films are improved, it would improve prospects for new technological applications illustrating that there are still unexplored aspects of the LbL technique.

Here we show for the first time LbL assembly of the simplest structured films with one charge per main chain carbon atom from the polymethylene-type polyelectrolytes, PF and PMA. These polyelectrolytes possess unusually strong side-chain interactions due to the high density of side-chain groups. Furthermore, the pK_a value of PF decreases from the corresponding solution value when incorporated in multilayer thin films. These features significantly affect the LbL assembly process, which facilitates prediction of the pH dependency of the assembly process in the range of dipping solution at pH 4.0−10.5.

Experimental Section

Materials. Poly(fumaric acid) (PF) was synthesized from poly(di-*tert*-butyl fumarate)[14] (M_w = 19 000, M_n = 8800) by pyrolysis, which quantitatively releases isobutene. Poly(methyleneamine) (PMA) was obtained as a HCl salt form using a modified synthetic route.[13] Starting from poly(1,3-diacetyl-4-imidazoline-2-one) (M_w = 45 000, M_n = 26 000), prepared by radical polymerization of imidazoline-2-one derivative,[15] hydrolysis of the cyclic urea units with aqueous NaOH, followed by the protonation with aqueous HCl furnished PMA as HCl salts. Because of the poor solubility of PF and PMA in common GPC solvents such as $CHCl_3$ and THF, the molecular weights of PF and PMA were estimated to be M_w = 9500 and M_n = 4500 for PF and M_w = 15 600 and M_n = 9000 for PMA on the basis of the quantitative conversion from the corresponding precursor polymers. The quantitative conversion of the polymer reactions was confirmed by the ^{1}H NMR and IR measurements of PF and PMA. Other reagents were used as received.

Determination of pK_a Values. pK_a values of the polyelectrolytes in solution were determined by potentiometric titration. Titration was performed with a glass/reference electrode calibrated with buffer solutions of pH 4.0, 7.0, and 9.0 for an acidic polymer solution of 6.25 mM by adding the 0.1 M standard NaOH solution with a microbiuret under nitrogen at 30 ± 0.1 °C. As the rate of equilibrium attainment was found to be rather slow, the titration was performed until pH values became constant for each step. The initial volume of the polymer solution was 80 mL.

The pK_a value of PF in the solid state was determined by FT-IR measurements. FT-IR spectra were recorded on a JASCO FT/IR-4100 infrared spectrophotometer. Aqueous solutions of PF, prepared similarly to those used for the multilayer dipping by adjusting the pH with aqueous HCl or aqueous NaOH, were cast onto a ZnSe substrate and evaporated under vacuum to yield polymer films. For the FT-IR analysis of PF in the form of a dried cast film, the two distinct absorption bands of carboxylate moieties were observed: ν = 1589−1578 cm^{-1} (asymmetric stretching band of COO^-) and ν = 1730−1720 cm^{-1} (C=O stretching band of COOH). Band intensities were normalized to the maximum peak height of each absorption spectrum. Assuming the same extinction coefficient for both bands, the degree of ionization (α) at a given pH can be calculated from $\alpha = [\nu(COO^-)]/[\nu(COOH) + \nu(COO^-)] \times 100$ (%).

Dipping Procedures. The silicon wafer (the thickness of the silica layer was about 300 nm: hereafter denoted as a Si wafer) was treated by using a UV-ozone cleaner (Nihon Laser Denshi, Co., Ltd.) for 2 h for preparation of the hydrophilic surface.

Dipping solutions of the polyelectrolytes were prepared at a concentration of 10^{-2} M (with respect to the macromolecular repeat unit) in 18 MΩ Millipore water, and the pH values were further adjusted with either aqueous HCl or aqueous NaOH as required. Additional salts were added to neither the polymer solutions nor rinse solutions. Layer-by-layer (LbL) deposition was carried out by using an automatic dipping machine (a programmable slide stainer). This dipping machine can be programmed to immerse a substrate into a series of up to 20 different solutions. The substrate was dipped into a polyelectrolyte solution followed by three agitated rinses in three separate bins of pH neutral water (pH of 5.5−6.5). The substrate was then dipped into the oppositely charged polyelectrolyte solution followed by the same rinsing procedure. The dipping time in the polyelectrolyte and water rinse solutions was 15 and 2 min, respectively (the final water rinse time was only 1 min). No drying step was used in the automatic dipping procedure. This procedure was repeated (alternating between polycation and polyanion) until 20 layers were deposited (i.e., 10 bilayers).

Quarts Crystal Microbalance (QCM) Measurements. An AT-cut quartz crystal with a parent frequency of 10 MHz was obtained from Crystal Sunlife (Japan). The crystal (9 mm diameter) was coated on both sides with mirror-like polished silver electrodes (5.5 mm diameter). The quartz substrates were ultrasonically agitated in an H_2O/EtOH (2:3) solution of KOH for 5 min and then ultrasonically washed with deionized water for 5 min × 2. The frequency was monitored using a universal counter (Hewlett-Packard). The leads of the QCM were protected with a silicon rubber gel to prevent degradation during immersion in the aqueous salt and organic solutions. The amount of polymer adsorbed, Δm, was calculated from the frequency decrease in the QCM, ΔF, using the Sauerbrey equation[16] as follows:

$$-\Delta F = \frac{2F_0^2}{A\sqrt{\rho_q \mu_q}}\Delta m \qquad (1)$$

where F_0 is the parent frequency of the QCM (1×10^7 Hz), A is the electrode area (0.237 cm^2), ρ_q is the density of the quartz (2.65 g cm^{-3}), and μ_q is the shear modulus (2.95×10^{11} dyn cm^{-2}). This equation is reliable even when measurements are performed in air. Since the mass of the solvents is never detected as a frequency shift, the effect of the adsorbent viscosity on the frequency can be neglected.

Spectroscopic Ellipsometry. The thickness and refractive index of the multilayer thin films fabricated on a polished Si wafer were determined by using ellipsometry (ESM-1A model from ULVAC) at 632 nm.

Atom Force Microscopy (AFM) Measurements. AFM images were taken of air-dried films using an SPA400-SPI4000 (Seiko Instruments Inc., Chiba, Japan) in dynamic force mode (DFM mode, i.e., tapping mode) using silicon cantilevers with a resonance frequency of ca. 128−137 kHz (SI-DF20, Seiko Instruments Inc.). Several images were taken on macroscopically separated areas of the films to ensure representative AFM images of the samples.

Fourier Transform Infrared Reflection Absorption Spectra (FT-IR-RAS) Measurements. FT-IR-RAS spectra of the LbL multilayer films assembled on a Si wafer were recorded on a Nicolet NEXUS 670FT-IR equipped with an MCT detector.

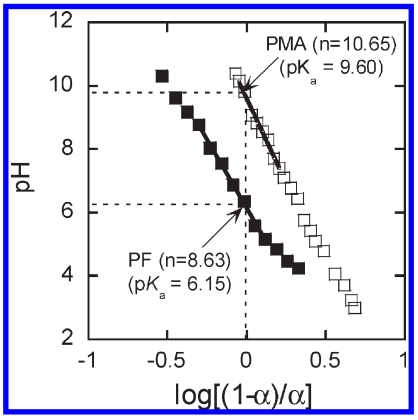

Figure 1. Henderson−Hasselbach plots of PF (■) and PMA (□) obtained by potentiometric titration.

Forty scans were collected for each spectrum at 2 cm^{-1} spectral resolution and 0.5 cm^{-1} interval.

Results and Discussion

Determination of Polyelectrolyte pK_a. It is well-known that the degree of ionization of weak polyelectrolytes significantly affects the LbL adsorption behaviors. Therefore, we initially performed potentiometric titrations to estimate the acid dissociation constants (pK_a) of poly(fumaric acid) (PF) and poly(methyleneamine) (PMA) as well as the interactions between the neighboring ionized groups of the polyelectrolytes in aqueous solutions. Homogeneous aqueous solutions of the polyelectrolytes containing 0.1 M $NaNO_3$ were prepared at a concentration of 6.25 mM/repeat unit. The pH change was recorded after each addition of 0.1 M NaOH solution and analyzed using the Henderson−Hasselbach equation (eq 2).[17]

$$\mathrm{pH} = \mathrm{p}K_a - n \log[\alpha/(1-\alpha)] \quad (2)$$

Here, pK_a is the intrinsic dissociation constant, and α is the degree of dissociation. The parameter n is a measure of the interactions between the neighboring ionized groups of the polyelectrolytes. When the main chain is not highly hydrophobic, this parameter substantially represents the magnitude of the electrostatic repulsion between charged side chain groups.

Figure 1 shows the Henderson−Hasselbach plots of PF and PMA. From these plots, the pK_a values of PF and PMA were determined to be 6.15 and 9.60, respectively. Although the pK_a of PMA has not been reported, the values of PF, prepared by radical polymerization of bis(trimethylsilyl)-fumarate followed by deprotection of the silyl substituents, had previously been reported by Kawaguchi et al.[18] They observed the two-step dissociations of PF by using infrared and UV spectroscopies as well as potentiometric titration. In contrast, we did not observe any well-defined stepwise dissociation in the measurement pH range. This might reflect differences in polymer configuration due to the differing synthetic routes. We used di-*tert*-butyl fumarate as a monomer for the radical polymerization, which presumably yields the corresponding PF with fewer intramolecular hydrogen-bonding interactions, and so a single-stepped dissociation was observed. The determined pK_a value of PF is similar or slightly acidic relative to the corresponding vinyl polymer, namely poly(acrylic acid) (pK_a ~ 6.8).[19] This is also true for PMA. The pK_a of PMA was close to or slightly higher than that of poly(allylamine) (pK_a ~ 8.9).[20] These results suggest that acid dissociation of the polymethylene-type polymer side chains occurs in a similar pH region to the corresponding vinyl polymers when measured in aqueous solutions. However, we found a remarkable difference in the n values between polymethylene-type polymers and vinyl polymers. The n values of PF and PMA determined from the Henderson−Hasselbach plots were 8.63 and 10.6, respectively, whereas the values of the corresponding vinyl polymers, poly(acrylic acid) and poly(allylamine), were ca. 2.2 and 2.0, respectively. These n values of polymethylene-type polymers are, to the best of our knowledge, some of the highest values ever reported. These values strongly suggest the large intramolecular electrostatic interactions existing between the polymer side chains. The dramatic increase in the n value by a factor of 6−9 is remarkable given that density of the functional groups in PF and PMA is just double that of the corresponding vinyl polymers. This increase will affect the intramolecular interactions between side chain groups via electrostatic repulsion and hydrogen-bonding formation as well as influence the morphology of single polymer chains and accordingly the LbL assembly process.

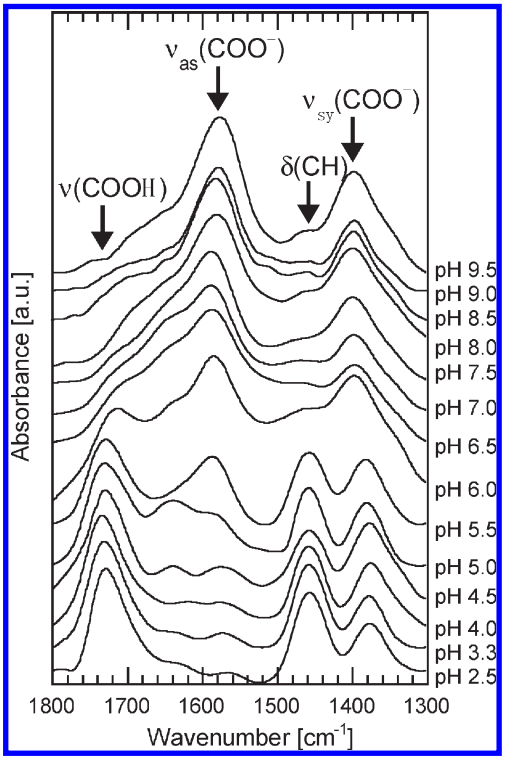

Figure 2. FT-IR spectra of PF films cast from aqueous solutions at various pH values onto a ZnSe substrate.

We then analyzed the dry films of each polymethylene-type polymer, PF and PMA, by using FT-IR spectroscopy, since the apparent dissociation constants of weak polyelectrolytes shift from their solution values when they are in the solid state or incorporated into LbL multilayer thin films.[21] In order to reveal the detailed assembly behaviors of oppositely charged polyelectrolytes, it is important to know the difference in acid dissociation constants between aqueous solution and solid film. Fortunately, the ionization degree of the polymer films can often be calculated from the amounts of ionized vs nonionized functional groups determined by FT-IR spectra.[22]

PF cast films prepared from aqueous solutions of different pH revealed two well-defined sets of C=O peaks in the range of 1800−1300 cm^{-1}. One is characteristic of the ionized COO^- symmetric and asymmetric vibrations, and the other is due to nonionized COOH (Figure 2). We employed the asymmetric COO^- peak at 1589−1578 cm^{-1} and COOH

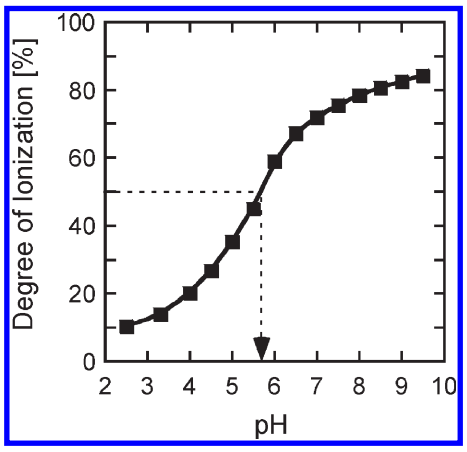

Figure 3. Estimated degree of ionization of PF solid film as a function of cast solution pH. Broken arrow represents the pH at which 50% of the PF units are charged (pK_a = 5.6).

peak at 1730−1720 cm^{-1} for estimation of the pK_a value, under the assumption that the extinction coefficients of both peaks are constant during the measurements. In the acidic region at pH 2.0, only the peak due to COOH could be detected, indicating essentially 100% acidic form (much below the pK_a). As solution pH was increased, the intensity of the COOH peak decreased with a corresponding increase in the intensity of the COO^- band. At pH 9.5, most of the carboxyl groups were deprotonated to the COO^- form. Figure 3 shows the degree of ionization in the solid film state of PF determined by FT-IR. From these plots, the pK_a of the single-component solid PF was determined to be about 5.6. This value is slightly lower than that observed in aqueous solution (6.15). In homogeneous aqueous solutions, pK_a of weak polymer acids tends to decrease with increasing COOH density, e.g., going from poly(acrylic acid) to PF. In other words, the result of more interactions between COOH groups is a lower pK_a. In solid-state PF, the intermolecular interactions between COOH groups become more significant, in addition to the greater intramolecular interactions, and accordingly, there is a further decrease in the pK_a. In the case of vinyl polymer acids, apparent decrease in the degree of dissociation is not usually observed in the single-component solid states. Thus, this observation is supposed to be a specific feature of polymethylene-type polyelectrolytes. PF might behave as a much stronger acid in the LbL assembly process because of the presence of the counter bases.

On the other hand, characteristic IR peaks suitable for the estimation of the acid dissociation constant could not be located in spectra of PMA solid films because of overlap with other peaks. In the case of poly(allylamine), the methylene ($-CH_2-$) vibration of the polymer main chain has been employed for normalization of all peak intensities.[22] However, spectra of PMA do not possess this methylene peak.

QCM Measurements. LbL deposition on a Si substrate was then analyzed using the QCM technique. Stepwise film fabrication was monitored as a function of the layer number by recording the frequency change ($-\Delta F$), which is related to the adsorbed mass according to the Sauerbrey equation.[16] The decrease in the resonance frequency of the QCM provides a measure of the adsorbed mass for each deposition step. Figure 4 displays one example of the dependence of frequency shifts in the assembly step when a QCM was alternately immersed in a pH 4.0 PF solution and a pH 10.5 PMA solution at 20 °C, the conditions that afforded the thickest film (vide infra). The plots clearly show the efficient alternate adsorption of both PF and PMA. However, there is

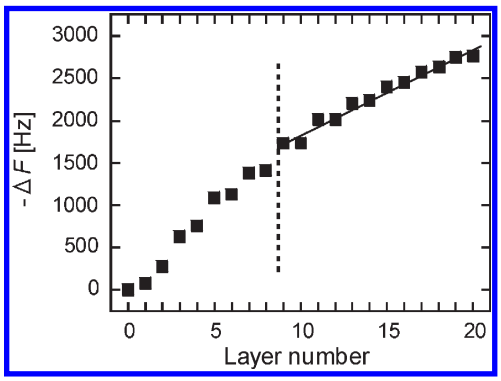

Figure 4. Frequency changes against the layer number for QCM measurements performed in a pH 4.0 PF solution (even layer number) and a pH 10.5 PMA solution (odd layer number) at 20 °C.

no linearity of the adsorption behavior up to four bilayers, probably because of the slight mismatching of the unevenness of the Si surface and the morphology of the polyelectrolytes used. After five bilayers, the plots show a linear behavior, implying the regular adsorption at the smooth LbL surfaces. This stepwise change in the alternate adsorption behavior at the stage of 4−5 bilayers was previously observed for the LbL combination of poly(allylamine) and poly(acrylic acid).[23] Thus, it was shown that the combination of PMA/PF is also suitable for LbL thin film fabrication based on these highest possible density polyelectrolytes and that 10 bilayers are sufficient for qualitative comparison of the resultant films.

pH Effect on LbL Thin Film Fabrication. For acquisition of reliable and reproducible data, an automatic dipping instrument was used to fabricate PMA/PF multilayer thin films on a Si wafer. The pH values of PF and PMA dipping solutions were systematically varied in the range of 4.0−10.5, where the polymers had been completely dissolved in water at a concentration of 10 mM/repeat unit. PF and PMA were rapidly deposited from the aqueous solutions at this concentration and a pH of ca. > 10 and ca. < 2, respectively. The pH range was also chosen in order to include the solution pK_a of both polymers (PF: 6.15 and PMA: 9.60).

Film thicknesses and refractive indices of the thin films were determined by spectroscopic ellipsometry. Reliability of the values was confirmed by the repeated preparation of the LbL thin films. Figure 5 shows the full pH matrix of these two parameters. This figure illustrates the effect of the dipping solution pH value on the multilayer thin film formation based on the assembling bilayer building blocks (dried films of polycation plus polyanion). A survey reveals that the deposition of the layer pair is dramatically influenced by the pH of the individual dipping solutions. This behavior is similar to poly(allylamine)/poly(acrylic acid) multilayer thin films, in which both electrostatic interactions and hydrogen bonding play a complementary and crucial role in LbL thin film formation, and the relationship between polymer structure and film morphology can be well accounted for by segmental repulsion effects.[24] In previous studies, the efficiency of polymer adsorption was usually judged from the film thickness, and it is concluded that a combination of a fully charged polycation with a partially charged polyanion, or vice versa, is more suitable for efficient LbL deposition than a combination of fully charged polycation and polyanion.[10,24] Efficient LbL deposition driven by hydrogen-bonding interactions has also been reported for almost neutral polymer combinations.[11] In accordance with these observations, the thickest film was obtained for the LbL preparation using pH 10.5 PMA solution and pH 4.0 PF

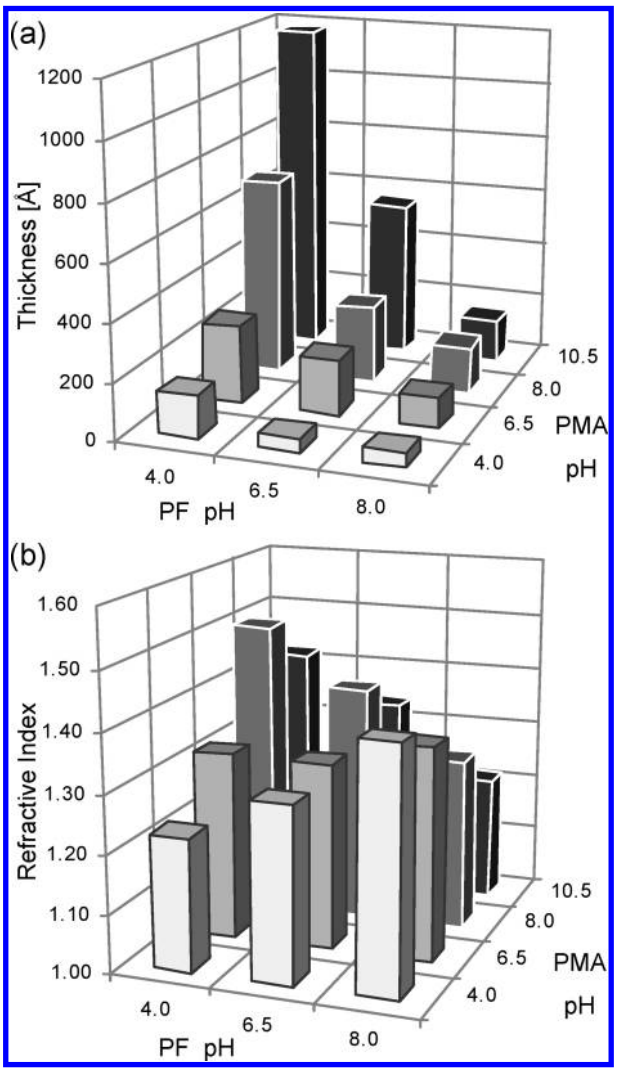

Figure 5. Complete pH matrix of (a) film thicknesses and (b) refractive indices of the PMA/PF 10 bilayers, as a function of dipping solution pH, determined by spectroscopic ellipsometry.

solution. In the dipping solutions, both PMA and PF are almost neutral. However, when they were deposited on the LbL thin film surface, it is thought that the pK_a value of PMA increased and that of PF decreased relative to each solution value, reaching a suitable charge balance. The 10-bilayer film thickness determined by ellipsometry measurement was 1183 Å. The film thickness gradually decreased with decreasing PMA pH and increasing PF pH and the thinnest film, of thickness 50 Å, was eventually obtained by the combination of a pH 4.0 PMA solution with a pH 8.0 PF solution. In this case, both polyelectrolytes should be almost fully charged in both dipping solutions and solid states, offering only the electrostatic attractions of fully extended rigid polymer chains for LbL deposition. These results suggest that the bilayer thicknesses of the PMA/PF LbL thin films can be controlled from 5 to 118 Å simply by adjusting the dipping solution pH. The maximum and minimum thicknesses are similar to those reported previously for the vinyl polyelectrolytes, but it should be emphasized that the pH dependence of the polymethylene-type polyelectrolytes is much clearer than in the conventional vinyl polyelectrolytes. Thus, LbL thin films with required thicknesses can be readily prepared by using the polymethylene-type polymers.

The degree of ionization was found to be one of the most important factors in the optimization of LbL adsorption efficiency of polymethylene-type polyelectrolytes. In seeking other factors, the LbL thin films composed of vinyl polyelectrolyte and polymethylene-type polyelectrolyte were also prepared by using a polycation dipping solution pH of 10.5 and polyanion dipping solution pH of 4.0, and the results were compared as a measure of the film thickness. In the case of the combination of PMA and poly(acrylic acid), the 10-bilayer film was 691 Å thick, whereas the combination of poly(allylamine) and PF provided a 10-bilayer film of thickness 535 Å. These film thicknesses are almost half those of the PMA/PF combinations. For the film prepared from a poly(allylamine) dipping solution pH of 8.5 and a poly(acrylic acid) dipping solution pH of 3.5−4.5, a bilayer thickness around 90 Å was reported (i.e., ∼900 Å for a 10-bilayer film).[24] Thus, polymethylene-type polyelectrolytes are less compatible with other differently structured polymer main-chain polyelectrolytes (a feature also true for vinyl polyelectrolytes). These results indicate the great importance of polymer structural design and selection for optimal pairing in the LbL process.

The above discussion is based on the assumption that the amount of polymer adsorbed is proportional to the film thickness. In other words, thicker films are generally composed of more polymers, although the flexible main chain of noncharged polymers has a larger hydrodynamic radius. Previously, the validity of this relationship was qualitatively demonstrated for multilayer thin films of positively charged TiO_2 and negatively charged SiO_2 nanoparticles by comparison of the film thickness and refractive index.[25] However, to the best of our knowledge, there have been no systematic studies on the refractive indices of weak polyelectrolyte LbL thin films as a function of the dipping solution pH values. Therefore, the characteristic behavior in the LbL thin film formation of polymethylene-type polyelectrolytes was also analyzed by the pH matrix profile of the refractive indices. A high refractive index qualitatively suggests well-packed or dense film while a low refractive index suggests coarsely assembled films with a certain amount of void space.[26] LbL thin films of conventional organic polyelectrolytes usually display low refractive indices.[27] Thus, the refractive indices of the obtained LbL films composed of the polymethylene-type polyelectrolytes ranged from 1.2 to 1.5. It should be noted that the pH matrix of refractive indices is completely different from that of film thicknesses (Figure 5). In Figure 5b, there are two peak maxima in the pH matrix. One relates to the film prepared from a PMA dipping solution of pH 8.0 and a PF dipping solution of pH 4.0. The other is due to the film prepared from a PMA dipping solution of pH 4.0 and a PF dipping solution of pH 8.0. The former is the combination of partially charged PMA (polycation)/neutral PF in the dipping solutions. However, since it is known that the pK_a in the multilayer thin films shifts by a factor of 3−5,[22] the ideal charge balance of fully charged polycation and partially charged polyanion might have resulted. In contrast, the latter film is composed of the fully charged PMA (polycation) and PF (polyanion). This result indicates that partially charged polyelectrolytes strongly interact with almost neutral or noncharged polyelectrolytes at the interface, whereas fully charged polyelectrolytes prefer adsorption to the fully but oppositely charged polyelectrolytes. This tendency is clearly illustrated in Figure 5b. When the PMA dipping solution pH is 8.0 or 10.5, the partial amino moieties of PMA should be positively charged. With these partial positive charges in the films, the refractive indices of the LbL thin films increased with a decrease in the PF dipping solution pH. On the other hand, since PMA is almost fully charged at pH values significantly

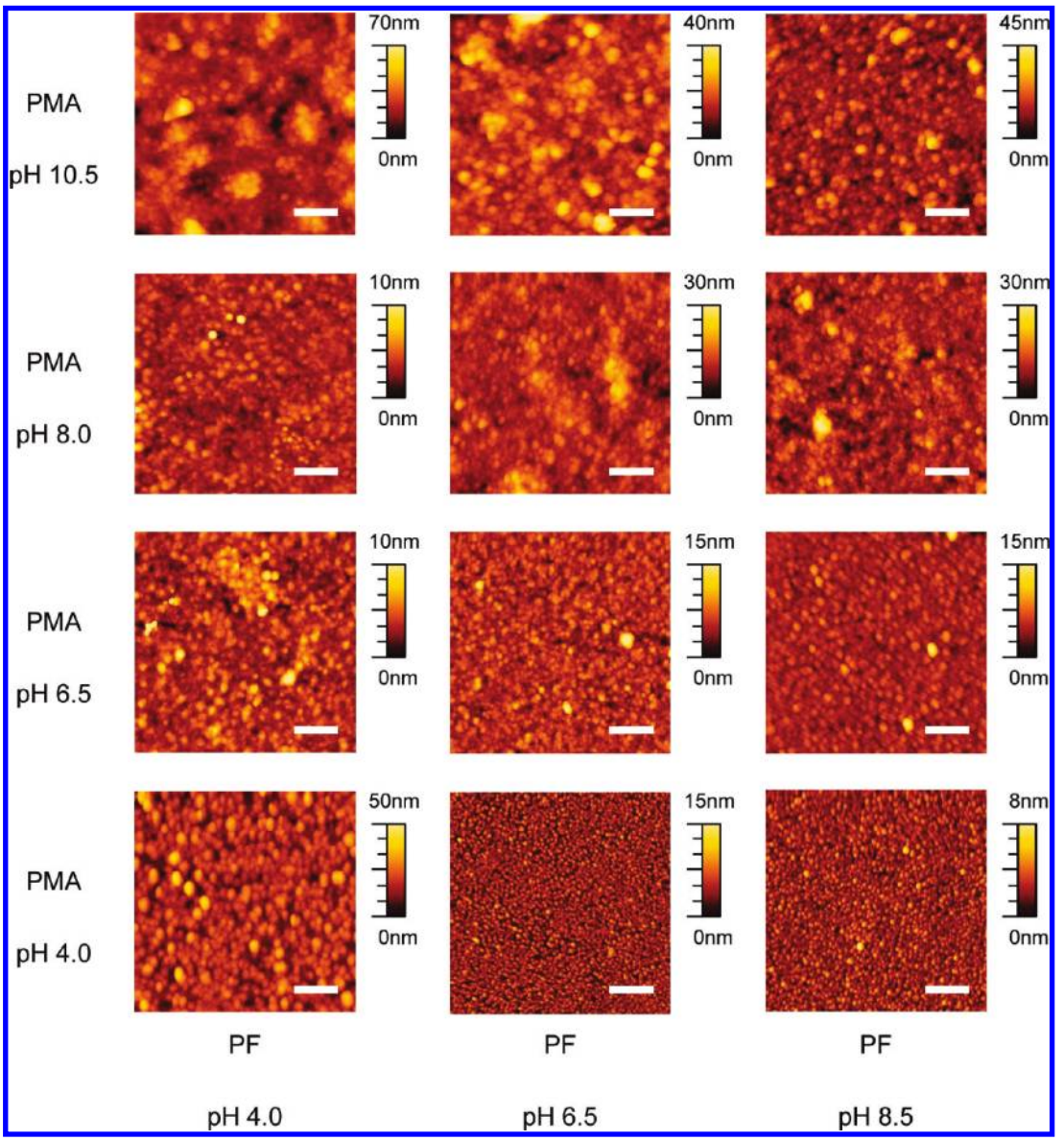

Figure 6. AFM images of PMA/PF 10-bilayer films prepared on Si substrates. From top to bottom: pH of PMA solutions shifts to acidity. From left to right: pH of PF solutions shifts to basicity. Scan size: 1 μm $\times$ 1 μm for all images. The white scale bar in each image represents 200 nm.

less than the pK_a, the refractive indices of the LbL thin films increased with the increasing PF dipping solution pH. This tendency becomes more significant when the PMA dipping solution pH is decreased from 6.5 to 4.0. This relationship is also true for PF. When the PF dipping solution pH was 4.0 or 6.5, the partially and negatively charged PF preferred almost neutral PMA rather than the positively charged PMA. However, as the PF dipping solution pH increased over the pK_a to 8.0, the fully charged PF altered its preference from the neutral to positively charged PMA. Thus, the LbL assembly of fully charged polyelectrolytes allowed the compact packing of the rigid polymer chains, resulting in the largest refractive index. Therefore, we conclude that the very thin films prepared in the LbL process do not always suggest the poor adsorption of the employed polyelectrolytes. However, judging from the relatively small difference in the refractive index values, it is also reasonable to say that the film thickness can be used for a qualitative assessment of the polymer adsorption efficiency.

AFM Measurements. Surface morphology of the 10-bilayer LbL thin films was investigated by using tapping mode AFM. The films prepared on a Si substrate were thoroughly dried under air. Figure 6 displays the AFM images taken by 1 μm $\times$ 1 μm size. As has been demonstrated in the film thickness and refractive index matrices obtained by spectroscopic ellipsometry, the surface morphology also exhibits a significant pH dependency. One notable feature is particle formation and their fusion at the Si surface. It is generally known that LbL thin films of strong polyelectrolytes are often composed of small polymer particles, which are formed by alternating self-assembly of oppositely charged rigid polyelectrolyte main chains in terms of the strong electrostatic interactions.[9a] Particle formation may also be attributed to the presence of small positively or negatively charged counterions (e.g., Na^+ and Cl^-, respectively).[28] On the other hand, a combination of weak polyelectrolytes tends to induce a fusion of the small polymer particles, leading to thicker LbL films with rough surfaces. This is mostly caused by the loop structures of partially or noncharged flexible polymer chains. It is also known that the phase transition in terms of the reorganization of weak polyelectrolytes within the thin films leads to a specific surface morphology.[29]

Polymethylene-type polyelectrolytes are basically weak polyelectrolytes because of the pH dependence of the charge densities, but the remarkably strong side-chain interactions, as demonstrated by the large n values in Henderson−Hasselbach plots, permit them serve provisionally as strong polyelectrolytes in specific pH regions. It is thought that these two effects operate simultaneously during the LbL thin film formation process.

When at least one of the polyelectrolytes was highly charged in the dipping solution, namely $> pK_a$ for PF and/or $< pK_a$ for PMA, a number of well-defined nanoparticles were observed (Figure 6). The particle size and distribution were dependent on the degree of ionization of the polyelectrolytes. Among the LbL thin films in this study, the film prepared from a PMA dipping solution of pH 4.0 and a PF dipping solution of pH 8.5 was made up of the finest particles with an average diameter of 17 nm. Under these preparation conditions, PMA and PF are supposedly highly charged polycations and polyanions, respectively, and act as strong polyelectrolytes. A polyelectrolyte should sense the shielding effect of electrostatic repulsion in the presence of the counter polyelectrolyte, which is similar to the effect of salt addition to strong polyelectrolyte solutions, leading to the nanoparticle formation. As the PMA dipping solution pH was increased and/or the PF dipping solution pH decreased, the particle size of the resulting assembled films became larger and finally became fused forming a rough surface. This fusion process is most pronounced when the polyelectrolyte pH exceeds the pK_a values in the dipping solutions. At a constant PMA dipping solution pH of 4.0, the observed average particle size increased significantly from ca. 17 to 42 nm when the PF dipping solution pH was changed from 6.5 to 4.0 (Figure 6). The same phenomenon was observed for the PMA dipping solutions at a constant PF dipping solution pH of 8.5. Thus, PMA and PF are weak polyelectrolytes in this pH region, leading to thicker films. As a result, the fusion process is strongly associated with the film thickness depicted in Figure 5a.

We also evaluated the root-mean-square (rms) surface roughness of the AFM images. It is needless to say that rms values are dependent on many factors including scanning mode, size, speed, and substrate used.[30] Therefore, all conditions were maintained constant. The pH matrix of the roughness parameters is shown in Figure 7. The film prepared from the highly charged PMA/PF combination displayed the smallest rms value, implying a dense and well-packed assembly of polymer particles of narrow size distribution. On the other hand, the film prepared from a PMA dipping solution of pH 10.5 and a PF dipping solution of pH 4.0 was composed of a fused assembly of polymer particles, and accordingly the largest rms value was observed, probably due to entanglement of the polymer chains. Interestingly, values of this matrix appear inversely correlated with those of the refractive indices shown in Figure 5b. For example, refractive index gradually increases with increasing PMA dipping solution pH from 4.0 to 8.0 at a constant PF dipping solution pH of 4.0, whereas the corresponding rms values decreases in this order. The rms values should be proportional to the particle sizes in the region where well-defined polymer particles are observed. These results suggest that the density of larger polymer particles is low compared to that of the smaller polymer particles. However, both refractive index and rms value increase when the PF dipping solution pH decreases at a constant PMA dipping solution pH of 10.5. In this region, no well-defined particle shapes were observed in the AFM images, and hydrogen-bonding effects probably become dominant according to the Lavalla model.[31] Thus, although the matrix line at the PMA dipping solution pH of 10.5 is exceptional, the inverse correlation between refractive index and rms value is almost justified.

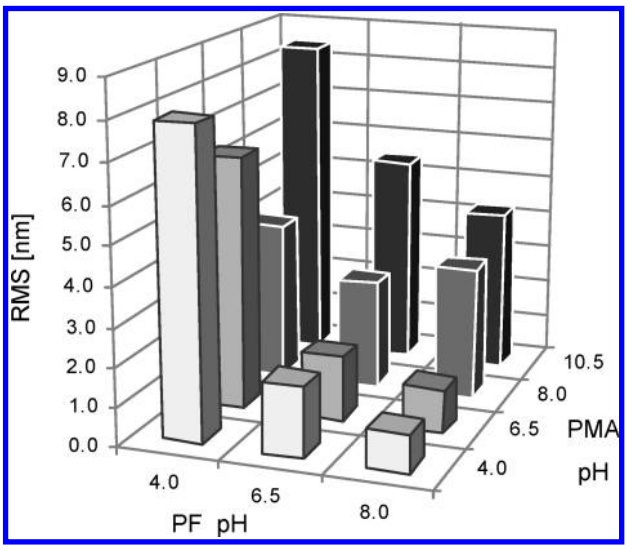

Figure 7. Complete pH matrix of rms values of the PMA/PF 10 bilayers as a function of dipping solution pH, determined by AFM.

FT-IR-RAS Measurements. It is important to obtain information on the apparent pK_a or degree of ionization in the multilayer thin films. In the previous studies using vinyl polyelectrolytes, it was reported that the pK_a of poly(acrylic acid) in the multilayer thin films decreases 3−5 pH units depending on the counter polycation species.[24,29,32] Figure 8 shows FT-IR-RAS spectra of the PMA/PF 10-bilayer films prepared on a Si substrate. The frequencies given in this Figure 8 correspond to the pH matrices of the thickness, refractive index, AFM, and rms values in Figures 5−7. The specific peaks of carboxylic acid and amine functions appeared in the range of 1800−1300 cm^{-1}. For example, a peak ascribed to the C=O function of PF carboxylic acid moieties was observed at 1690−1670 cm^{-1} for all the films. The peak position is much lower in energy than free carboxylic acids (typically at ca. 1750 cm^{-1}) and carboxylic acid dimers (typically at ca. 1720−1706 cm^{-1}). Single-component PF in the solid thin film state on a ZnSe plate displayed a C=O peak at 1720−1730 cm^{-1} (vide supra). Thus, the presence of PMA should further shift the peak position to lower energy due to hydrogen bonding. Similar behavior was previously reported for poly(acrylic acid) and other polymers bearing carboxylic acid groups.[22] The peak ascribed to NH_3^+ moieties of PMA was detected at 1498−1508 cm^{-1}.

As the PF dipping solution pH increased from pH 4.0 (Figure 8a) to 6.5 (Figure 8b), and further to 8.0 (Figure 8c), the relative intensity of the COOH peak decreased and the intensities of the COO^- peaks increased, indicating a larger contribution of electrostatic interactions to the film formation. It is remarkable that the COO^- peaks clearly appeared even for the film prepared at the PF dipping solution pH of 4.0 (below the solution pK_a). In addition to hydrogen bonds, the presence of ammonium cations essentially facilitates the proton release of COOH groups or generation of COO^- groups. The degree of ionization of PF in the multilayer thin films was calculated from the relative intensities of these two bands. At the PMA/PF dipping solution pH of 4.0/8.0, the degree of ionization was 0.719. The value gradually decreased as the PF dipping solution pH decreased. Thus, the degree of ionization was 0.714 at the PMA/PF dipping solution pH of 4.0/6.5 and 0.569 at the PMA/PF dipping

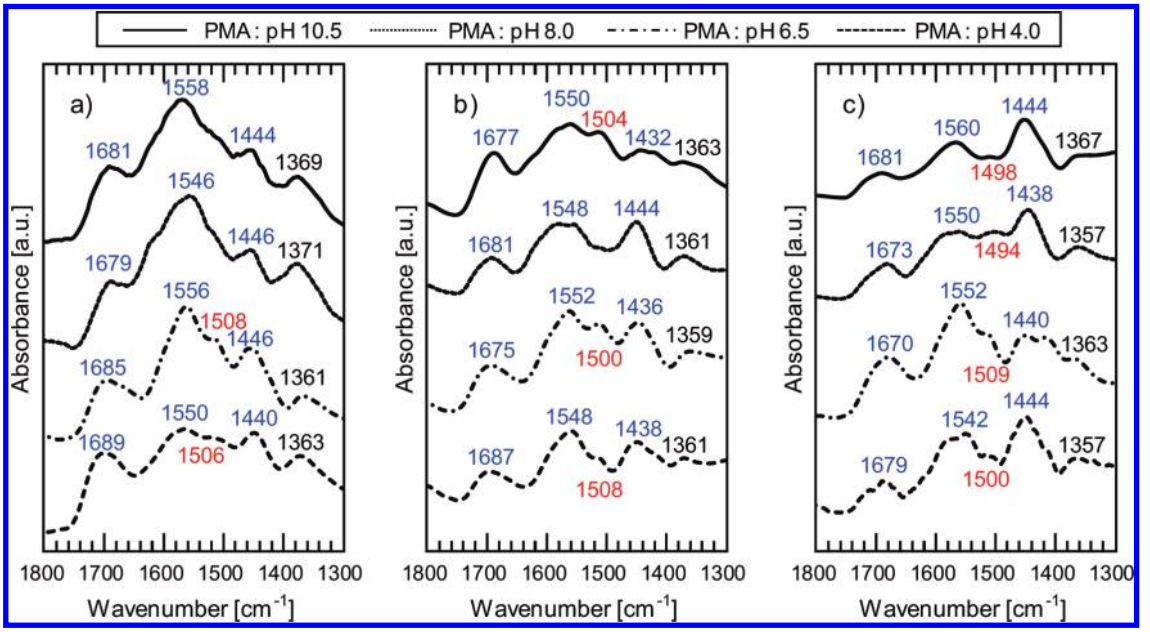

Figure 8. FT-IR-RAS spectra of PMA/PF 10-bilayer films on a Si substrate, prepared from various polyelectrolyte solutions with different pH values: (a) PF solution at pH of 4.0, (b) PF solution at pH of 6.5, and (c) PF solution at pH of 8.0. The spectra were offset in the positive direction for clarity. The color code is as follows: ν = 1357−1369 cm^{-1} (CH skeletal deformation vibration), black; ν = 1498−1508 cm^{-1} (NH_3^+ bending vibration), red: ν = 1432−1446 cm^{-1} (COO^- symmetrical stretching vibration), 1542−1560 cm^{-1} (COO^- asymmetrical stretching vibration), and 1670−1689 cm^{-1} (C═O stretching vibration of carboxylic acid), blue.

solution pH of 4.0/4.0. These behaviors are almost comparable to those reported for the poly(allylamine)/poly(acrylic acid) combination, which showed a pK_a decrease of 4.5 pH units in the multilayer thin film when compared to the solution pK_a.[22] Unfortunately, the apparent pK_a of PF in the multilayer thin film could not be determined because of the limited availability of PF. However, taking into account a similar pK_a decrease in the vinyl polyelectrolytes, it is estimated to be ca. 2.

The peak intensities of NH_3^+ became stronger as the PF dipping solution pH increased and PMA dipping solution pH decreased. The former is ascribed to the charge compensation and the latter to the original feature of PMA. It is difficult to discuss further the degree of ionization and pK_a in the multilayer because of the large degree of overlap of the peaks in the FT-IR spectra. However, if we suppose that a well-defined NH_3^+ peak could not be observed with a PMA dipping solution pH of 10.5 and lower PF dipping solution pH, the apparent pK_a of PMA in the multilayer might be similar to the solution value. This idea is partially substantiated by the abrupt transition in the AFM images and the rms profiles when the PMA dipping solution pH exceeded the solution pK_a in the range from 8.0 to 10.5 or vice versa.

Conclusions

We have investigated a hitherto unexplored fundamental research field of LbL science by using polymethylene-type polyelectrolytes, PF and PMA, which are respectively the *structurally simplest* of the available polyanions and polycations, and also possess the *highest charge densities*. The pK_a values for PF and PMA, determined by potentiometric titrations and FT-IR spectroscopy as well as the LbL assembly behavior determined by QCM frequency shifts, were similar to the corresponding vinyl polyelectrolytes. However, the specific feature of the double charge densities of PF and PMA (over the corresponding vinyl-type polyelectrolytes) was detected as the extremely large electrostatic side chain interactions, as demonstrated by the Henderson−Hasselbach plots. These stronger electrostatic interactions and the double density of the side-chain charges enable the polymethylene-type polyelectrolytes to serve not only as weak polyelectrolytes but also partially as strong polyelectrolytes. AFM measurements permitted clear visualization of this transition from a well-ordered dense packing of monodispersed nanoparticles for the fully charged PMA/PF combination to a rough surface composed of fused nanoparticles for the partially charged PMA/PF combination. Moreover, the relationship between refractive index and roughness parameter for the AFM images was revealed for the first time. It was found that the pH matrix of refractive indices also provides information on the polymer adsorption and that these parameters are not directly associated with the film thickness. Therefore, it should be noted that thin films do not always indicate poor LbL adsorption.

A diverse range of polymethylene-type polyelectrolyte derivatives can be designed and readily synthesized on a large scale. The smooth and predictable variation of film thickness in the pH matrix offers the great utility of the polymethylene-type polyelectrolytes for technological applications.

Acknowledgment. This work was supported, in part, by a Grant-in-Aid for Scientific Research, the Special Coordination Funds for Promoting Science and Technology from MEXT, Japan, World Premier International Research Center Initiative (WPI Initiative), MEXT, Japan, and Core Research for Evolutional Science and Technology (CREST) program of Japan Science and Technology Agency (JST).

References and Notes

(1) For reviews, see: (a) Philipp, B.; Dautzenberg, H.; Linow, K.-J.; Kotz, J.; Dawydoff, W. *Prog. Polym. Sci.* **1989**, *14*, 91. (b) Decher, G. *Science* **1997**, *277*, 1232. (c) Hammond, P. T. *Adv. Mater.* **2004**, *16*, 1271. (d) Jiang, C.; Tsukruk, V. V. *Adv. Mater.* **2006**, *18*, 829. (e) Ariga, K.; Hill, J. P.; Ji, Q. *Phys. Chem. Chem. Phys.* **2007**, *9*, 2319. (f) Quinn, J. F.; Johnston, A. P. R.; Such, G. K.; Zelikin, A. N.; Caruso, F. *Chem. Soc. Rev.* **2007**, *36*, 707. (g) Quinn, A.; Such, G. K.; Quinn, J. F.; Caruso, F. *Adv. Funct. Mater.* **2008**, *18*, 17. (h) Ariga, K.; Hill, J. P.; Lee, M. V.; Vinu, A.; Charvet, R.; Acharya, S. *Sci. Technol. Adv. Mater.* **2008**, *9*, 014109. (i) Lichter, J. A.; Van Vliet, K. J.; Rubner, M. F. *Macromolecules* **2009**, *42*, 8573.

(2) (a) Lvov, Y.; Decher, G.; Möhwald, H. *Langmuir* **1993**, *9*, 481. (b) Serizawa, T.; Hamada, K.; Akashi, M. *Nature* **2004**, *429*, 52. (c) Morgan, S. E.; Jones, P.; Lamont, A. S.; Heidenreich, A.; McCormick, C. L. *Langmuir* **2007**, *23*, 230. (d) South, C. R.; Piñón, V.III; Weck, M. *Angew. Chem., Int. Ed.* **2008**, *47*, 1425. (e) Lee, H.; Lee, Y.; Statz, A. R.; Rho, J.; Park, T. G.; Messersmith, P. B. *Adv. Mater.* **2008**, *20*, 1619.

(3) (a) Lvov, Y.; Ariga, K.; Ichinose, I.; Kunitake, T. *J. Chem. Soc., Chem. Commun.* **1995**, 2313. (b) Caruso, F.; Trau, D.; Möhwald, H.; Renneberg, R. *Langmuir* **2000**, *16*, 1485. (c) Lu, G.; Ai, S.; Li, J. *Langmuir* **2005**, *21*, 1679. (d) Wang, Y.; Angelatos, A. S.; Caruso, F. *Chem. Mater.* **2008**, *20*, 848. (e) Dronov, R.; Kurth, D. G.; Möhwald, H.; Spricigo, R.; Leimkühler, S.; Wollenberger, U.; Rajagopalan, K. V.; Scheller, F. W.; Lisdat, F. *J. Am. Chem. Soc.* **2008**, *130*, 1122. (f) Wilson, R.; Mehrabi, M.; Prior, I. A.; Beckett, A.; Hutchinson, A. *Chem. Commun.* **2009**, 2487.

(4) (a) Lvov, Y.; Essler, F.; Decher, G. *J. Phys. Chem.* **1993**, *97*, 13773. (b) Cooper, T. M.; Campbell, A. L.; Crane, R. L. *Langmuir* **1995**, *11*, 2713. (c) Ariga, K.; Lvov, Y.; Kunitake, T. *J. Am. Chem. Soc.* **1997**, *119*, 2224. (d) Maier, A.; Rabindranath, A. R.; Tieke, B. *Chem. Mater.* **2009**, *21*, 3668.

(5) (a) Jan, E.; Kotov, N. A. *Nano Lett.* **2007**, *7*, 1123. (b) Michel, M.; Taylor, A.; Sekol, R.; Podsiadlo, P.; Ho, P.; Kotov, N.; Thompson, L. *Adv. Mater.* **2007**, *19*, 3859. (c) Shim, B. S.; Tang, Z.; Morabito, M. P.; Agarwal, A.; Hong, H.; Kotov, N. A. *Chem. Mater.* **2007**, *19*, 5467. (d) Lee, S. W.; Kim, B.-S.; Chen, S.; Shao-Horn, Y.; Hammond, P. T. *J. Am. Chem. Soc.* **2009**, *131*, 671.

(6) (a) Lvov, Y.; Ariga, K.; Ichinose, I.; Kunitake, T. *Langmuir* **1996**, *12*, 3038. (b) Schmitt, J.; Decher, G.; Dressick, W. J.; Brandow, S. L.; Geer, R. E.; Shashidhar, R.; Calvert, J. M. *Adv. Mater.* **1997**, *9*, 61. (c) Kotov, N. A.; Haraszti, T.; Turi, L.; Zavala, G.; Geer, R. E.; Dekany, I.; Fendler, J. H. *J. Am. Chem. Soc.* **1997**, *119*, 6821. (d) Caruso, F.; Lichtenfeld, H.; Giersig, M.; Möhwald, H. *J. Am. Chem. Soc.* **1998**, *120*, 8523. (e) Jaffar, S.; Nam, K. T.; Khademhosseini, A.; Xing, J.; Langer, R. S.; Belcher, A. M. *Nano Lett.* **2004**, *4*, 1421. (f) Li, L.; Ma, R.; Ebina, Y.; Fukuda, K.; Takada, K.; Sasaki, T. *J. Am. Chem. Soc.* **2007**, *129*, 8000. (g) Srivastava, S.; Kotov, N. A. *Acc. Chem. Res.* **2008**, *41*, 1831. (h) Nagaoka, Y.; Shiratori, S.; Einaga, Y. *Chem. Mater.* **2008**, *20*, 4004. (i) Liu, Q.; Yao, L.; Shen, Q.; Nie, Z.; Guo, M.; Yao, S. *Chem.—Eur. J.* **2009**, *15*, 12828.

(7) (a) Onda, M.; Lvov, Y.; Ariga, K.; Kunitake, T. *J. Ferment. Bioeng.* **1996**, *82*, 502. (b) Onda, M.; Ariga, K.; Kunitake, T. *J. Biosci. Bioeng.* **1999**, *87*, 69. (c) Zhou, L.; Yang, J.; Estavillo, C.; Stuart, J. D.; Schenkman, J. B.; Rusling, J. F. *J. Am. Chem. Soc.* **2003**, *125*, 1431. (d) Shchukin, D. G.; Patel, A. A.; Sukhorukov, G. B.; Lvov, Y. M. *J. Am. Chem. Soc.* **2004**, *126*, 3374. (e) Zhang, J.; Chua, L. S.; Lynn, D. M. *Langmuir* **2004**, *20*, 8015. (f) Tang, Z.; Wang, Y.; Podsiadlo, P.; Kotov, N. A. *Adv. Mater.* **2006**, *18*, 3203. (g) De Geest, B. G.; Sanders, N. N.; Sukhorukov, G. B.; Demeester, J.; De Smedt, S. C. *Chem. Soc. Rev.* **2007**, *36*, 636. (h) De Koker, S.; De Geest, B. G.; Cuvelier, C.; Ferdinande, L.; Deckers, W.; Hennink, W. E.; De Smedt, S. C.; Mertens, N. *Adv. Funct. Mater.* **2007**, *17*, 3754. (i) Nadiri, A.; Kuchler-Bopp, S.; Mjahed, H.; Hu, B.; Haikel, Y.; Schaaf, P.; Voegel, J.-C.; Benkirane-Jessel, N. *Small* **2007**, *3*, 1577. (j) Ji, Q.; Miyahara, M.; Hill, J. P.; Acharya, S.; Vinu, A.; Yoon, S. B.; Yu, J.-S.; Sakamoto, K.; Ariga, K. *J. Am. Chem. Soc.* **2008**, *130*, 2376. (k) Rusling, J. F.; Hvastkovs, E. G.; Hull, D. O.; Schenkman, J. B. *Chem. Commun.* **2008**, 141. (l) Crouzier, T.; Ren, K.; Nicolas, C.; Roy, C.; Picart, C. *Small* **2009**, *5*, 598. (m) Fujie, T.; Matsutani, N.; Kinoshita, M.; Okamura, Y.; Saito, A.; Takeoka, S. *Adv. Funct. Mater.* **2009**, *19*, 2560. (n) Okamura, Y.; Kabata, K.; Kinoshita, M.; Saitoh, D.; Takeoka, S. *Adv. Mater.* **2009**, *21*, 4388.

(8) (a) Serizawa, T.; Kawanishi, N.; Akashi, M. *Macromolecules* **2003**, *36*, 1967. (b) Kharlampieva, E.; Sukhishvili, S. A. *Langmuir* **2003**, *19*, 1235. (c) Cho, J.; Quinn, J. F.; Caruso, F. *J. Am. Chem. Soc.* **2004**, *126*, 2270. (d) Tjipto, E.; Quinn, J. F.; Caruso, F. *Langmuir* **2005**, *21*, 8785. (e) Tjipto, E.; Quinn, J. F.; Caruso, F. *J. Polym. Sci., Part A: Polym. Chem.* **2007**, *45*, 4341.

(9) (a) Schoeler, B.; Kumaraswamy, G.; Caruso, F. *Macromolecules* **2002**, *35*, 889. (b) Schoeler, B.; Sharpe, S.; Hatton, T. A.; Caruso, F. *Langmuir* **2004**, *20*, 2730.

(10) (a) Park, S. Y.; Rubner, M .F.; Mayes, A. M. *Langmuir* **2002**, *18*, 9600. (b) Itano, K.; Choi, J.; Rubner, M. F. *Macromolecules* **2005**, *38*, 3450. (c) Connal, L. A.; Li, Q.; Quinn, J. F.; Tjipto, E.; Caruso, F.; Qiao, G. G. *Macromolecules* **2008**, *41*, 2620.

(11) (a) Stockton, W. B.; Rubner, M. F. *Macromolecules* **1997**, *30*, 2717. (b) Clark, S. L.; Hammond, P. T. *Langmuir* **2000**, *16*, 10206. (c) Sukhishvili, S. A.; Granick, S. *Macromolecules* **2002**, *35*, 301. (d) Schoeler, B.; Poptoshev, E.; Caruso, F. *Macromolecules* **2003**, *36*, 5258. (e) Quinn, J. F.; Caruso, F. *Macromolecules* **2005**, *38*, 3414. (f) Kharlampieva, E.; Kozlovskaya, V.; Sukhishvili, S. A. *Adv. Mater.* **2009**, *21*, 3053.

(12) (a) Shigehara, K.; Hara, M.; Nakahama, H.; Miyata, S.; Murata, Y.; Yamada, A. *J. Am. Chem. Soc.* **1987**, *109*, 1237. (b) Fujii, N.; Michinobu, T.; Shigehara, K. *Chem. Lett.* **2007**, *36*, 1052. (c) Noguchi, H.; Michinobu, T.; Fujii, N.; Funahashi, M.; Tokita, M.; Watanabe, J.; Shigehara, K. *J. Polym. Sci., Part A: Polym. Chem.* **2008**, *46*, 5101. (d) Michinobu, T.; Fujii, N.; Tokita, M.; Watanabe, J.; Shigehara, K. *Macromol. Rapid Commun.* **2008**, *29*, 1593.

(13) Klapper, M.; Hamciuc, C.; Dyllick-Brenzinger, R.; Müllen, K. *Angew. Chem., Int. Ed.* **2003**, *42*, 4687.

(14) Otsu, T.; Yasuhara, T.; Shiraishi, K.; Mori, S. *Polym. Bull.* **1984**, *12*, 449.

(15) Baxter, R. L.; Camp, D. J.; Coutts, A.; Shaw, N. *J. Chem. Soc., Perkin Trans. 1* **1992**, 255.

(16) Sauerbrey, G. Z. *Z. Phys.* **1959**, *155*, 206.

(17) (a) Roux, C.; Bergeron, J. Y.; Leclerc, M. *Makromol. Chem.* **1993**, *194*, 869. (b) Faid, K.; Leclerc, M. *J. Am. Chem. Soc.* **1998**, *120*, 5274.

(18) (a) Kitano, T.; Kawaguchi, S.; Ito, K.; Minakata, A. *Macromolecules* **1987**, *20*, 1598. (b) Kitano, T.; Ishigaki, A.; Uematsu, G.-I.; Kawaguchi, S.; Ito, K. *J. Polym. Sci., Part A: Polym. Chem.* **1987**, *25*, 979. (c) Kawaguchi, S.; Kitano, T.; Ito, K. *Macromolecules* **1992**, *25*, 1294.

(19) Roma-Luciow, R.; Sarraf, L.; Morcellet, M. *Polym. Bull.* **2000**, *45*, 411.

(20) Crea, F.; Crea, P.; De Stefano, C.; Giuffrè, O.; Pettignano, A.; Sammartano, S. *J. Chem. Eng. Data* **2004**, *49*, 658.

(21) Rmaile, H. H.; Schlenoff, J. B. *Langmuir* **2002**, *22*, 8263.

(22) Choi, J.; Rubner, M. F. *Macromolecules* **2005**, *38*, 116.

(23) Fujita, S.; Shiratori, S. *Nanotechnology* **2005**, *16*, 1821.

(24) Shiratori, S. S.; Rubner, M. F. *Macromolecules* **2000**, *33*, 4213.

(25) Lee, D.; Omolade, D.; Cohen, R. E.; Rubner, M. F. *Chem. Mater.* **2007**, *19*, 1427.

(26) Wang, Z.; Heflin, J. R.; Stolen, R. H.; Ramachandran, S. *Appl. Phys. Chem.* **2005**, *86*, 223104.

(27) Kim, J.-H.; Fujita, S.; Shiratori, S. *Colloids Surf., A* **2006**, *284*, 290.

(28) (a) Schlenoff, J. B.; Ly, H.; Li, M. *J. Am. Chem. Soc.* **1998**, *120*, 7626. (b) Radeva, T. *Physical Chemistry of Polyelectrolytes*; Marcel Dekker: New York, 2001.

(29) Mendelsohn, J. D.; Barrett, C. J.; Chan, V. V.; Pal, A. J.; Mayes, A. M.; Rubner, M. F. *Langmuir* **2000**, *16*, 5017.

(30) Lobo, R. F. M.; Pereira-da-Silva, M. A.; Raposo, M.; Faria, R. M.; Oliveira, O. N., Jr. *Nanotechnology* **2003**, *14*, 101.

(31) Lavalle, P.; Gergely, C.; Cuisinier, F. J. G.; Decher, G.; Schaaf, P.; Voegel, J. C.; Picart, C. *Macromolecules* **2002**, *35*, 4458.

(32) (a) Yoo, D.; Shiratori, S. S.; Rubner, M. F. *Macromolecules* **1998**, *31*, 4309. (b) Burke, S. E.; Barrett, C. J. *Langmuir* **2003**, *19*, 3297.